J. Fluid Mech. (1993), *vol.* 255, *pp.* 183–194
Copyright © 1993 Cambridge University Press

Asymptotic theory of wall-attached convection in a rotating fluid layer

By J. HERRMANN AND F. H. BUSSE
Institute of Physics, University of Bayreuth, D-95440 Bayreuth, Germany

(Received 9 December 1992 and in revised form 5 April 1993)

Asymptotic expressions for the onset of convection in a horizontal fluid layer of finite extent heated from below and rotating about a vertical axis are derived in the limit of large rotation rates in the case of stress-free upper and lower boundaries. In the presence of vertical sidewalls, the critical Rayleigh number R_c is much lower than the classical value for an infinitely extended layer. In particular, we find that R_c grows in proportion to τ when the sidewall is insulating, where τ is the dimensionless rotation rate. When the sidewall is infinitely conducting, R_c grows in proportion to $\tau^{\frac{4}{3}}$ as in the case of an infinitely extended layer but with a lower coefficient of proportionality. Numerical results obtained at finite values of τ show good agreement with the asymptotic formulae.

1. Introduction

The problem of the critical conditions for the onset of convection in a rotating fluid layer heated from below has received much attention ever since Rossby (1969) noticed that in his experiment with a water layer the onset of convection occurred at a lower critical Rayleigh number than that predicted by the theory of Chandrasekhar (1961). In later experiments by Lucas, Pfotenhauer & Donnelly (1983) and by Pfotenhauer, Niemela & Donnelly (1987) a similar discrepancy was observed. At about the same time Buell & Catton (1983) found from numerical computations that in a circular layer of finite radius non-axisymmetric forms of convection could set in at Rayleigh numbers considerably below the value R_∞ calculated for an infinite layer. This finding appeared to resolve reasonably well the discrepancies between experimentally observed and theoretically predicted values. More recent detailed observations by Zhong, Ecke & Steinberg (1991) and by Ecke, Zhong & Knobloch (1991) have demonstrated, however, that the onset of convection occurs in the form of drifting waves in contrast to the steady modes assumed in the analysis of Buell & Catton. As has been pointed quite correctly by Ecke *et al.* time-dependent onset must be regarded as the rule rather than the exception in a rotating system because of the broken left–right symmetry. Detailed computations for the onset of drifting modes by Goldstein *et al.* (1993) show good agreement with the observations of Ecke *et al.*

The computations of Buell & Catton (1983) as well as the more recent calculations by Goldstein *et al.* (1993) have demonstrated that the presence of sidewalls supports the early onset of convection and that insulating sidewalls in particular lead to a substantial decrease in the critical Rayleigh number in comparison to the case of an infinite layer. But the range of the rotation parameter considered in the calculations has been restricted owing to the problems of numerical convergence, and because of the assumption of a circular layer the aspect ratio has entered the analysis as an additional

parameter. Since the wall-attached convection flow represents basically a boundary-layer phenomenon in terms of the distance from the sidewalls, a finite curvature of the wall is not an essential ingredient of the problem. In this paper an asymptotic analysis as well as a numerical study are presented for the case of a plane sidewall. A main result is the different power laws obtained for conducting and insulating sidewalls.

The mathematical formulation of the problem is given in §2. The asymptotic theory is derived in §3 and its analytical expressions are compared with numerical results obtained for finite values of the rotation parameter in §4. A general discussion is given in a concluding section.

2. Mathematical formulation of the problem

We consider a horizontal fluid layer heated from below with a vertical sidewall which is rotating about a vertical axis. We use the thickness d of the layer as lengthscale, d^2/κ as timescale where κ is the thermal diffusivity, and the temperature difference between lower and upper boundary, $T_2 - T_1$, as temperature scale. We introduce a Cartesian system of coordinates with the x-axis normal to the sidewall, the y-axis parallel to the sidewall and the z-coordinate in the vertical direction as indicated in figure 1. The unit vectors $\boldsymbol{i},\boldsymbol{j},\boldsymbol{k}$ point in the x-, y-, z-directions, respectively. For the solenoidal velocity field $\boldsymbol{v}$ we use the general representation

$$\boldsymbol{v} = \boldsymbol{\nabla} \times (\boldsymbol{\nabla} \times \boldsymbol{i}v) + \boldsymbol{\nabla} \times \boldsymbol{i}w. \tag{2.1}$$

By taking the x-components of the (curl)^2 and of the curl of the equations of motion in the rotating system, we obtain the following equations for v and w:

$$\left(\nabla^2 - P^{-1}\frac{\partial}{\partial t}\right)\nabla^2\Delta_2 v - \tau\frac{\partial}{\partial z}\Delta_2 w + R\frac{\partial^2}{\partial x\,\partial z}\theta = 0, \tag{2.2a}$$

$$\left(\nabla^2 - P^{-1}\frac{\partial}{\partial t}\right)\Delta_2 w + \tau\frac{\partial}{\partial z}\Delta_2 v - R\frac{\partial}{\partial y}\theta = 0, \tag{2.2b}$$

where θ describes the deviation of the temperature from the static solution of pure conduction. θ is determined by the heat equation

$$\left(\nabla^2 - \frac{\partial}{\partial t}\right)\theta + \frac{\partial^2}{\partial x\,\partial z}v - \frac{\partial}{\partial y}w = 0. \tag{2.2c}$$

We have neglected all nonlinear terms since we are interested in convection flows of infinitesimal amplitudes. The centrifugal force has been neglected in comparison with gravity and Δ_2 denotes the two-dimensional Laplacian, $\Delta_2 = \partial^2/\partial y^2 + \partial^2/\partial z^2$. The Rayleigh number R, the rotation parameter τ, and the Prandtl number P are defined by

$$R = \frac{\gamma g(T_2 - T_1)\,d^3}{\nu\kappa}, \quad \tau = \frac{2\Omega d^2}{\nu}, \quad P = \frac{\nu}{\kappa}, \tag{2.3}$$

where γ is the thermal expansivity, g is the acceleration due to gravity, ν is the kinematic viscosity, and Ω is the angular velocity of rotation. Note that the neglection of the centrifugal force in comparison with g can be justified even in the limit of large τ as long as g and d^2/ν are sufficiently large. For example, for a layer of water with a diameter of 1 m and a height $d = 10$ cm which is rotating with 6 r.p.m. the centrifugal force is 2% of gravity at the rim while τ is about 1.3×10^4.

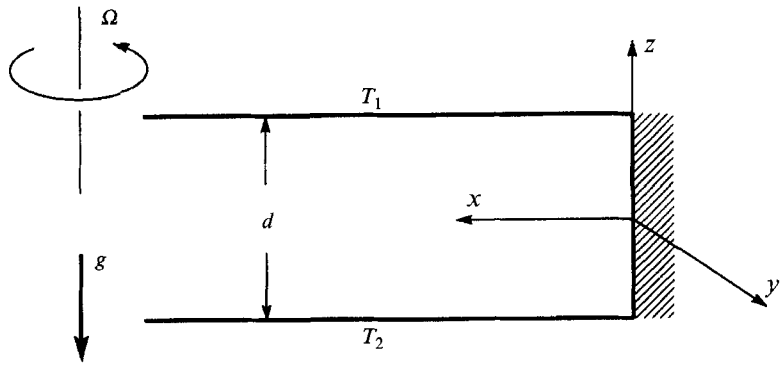

FIGURE 1. Geometrical configuration of the problem of wall-attached convection.

The boundary conditions at the stress-free upper and lower boundaries and at the rigid sidewall are given by

$$\frac{\partial}{\partial z}v = \frac{\partial^3}{\partial z^3}v = w = \frac{\partial^2}{\partial z^2}w = \theta = 0 \quad \text{at} \quad z = \pm\tfrac{1}{2}, \tag{2.4}$$

$$v = \frac{\partial}{\partial x}v = w = 0 \quad \text{at} \quad x = 0, \tag{2.5a}$$

$$\begin{Bmatrix} (\partial/\partial x)\,\theta \\ \theta \end{Bmatrix} = 0 \quad \text{for} \quad \begin{Bmatrix} \text{insulating: case I} \\ \text{conducting: case C} \end{Bmatrix} \text{sidewall} \quad \text{at} \quad x = 0. \tag{2.5b}$$

The combination of stress-free boundaries at $z = \pm\frac{1}{2}$ and a no-slip boundary at $x = 0$ offers the advantage that separable solutions of the linear problem (2.3), (2.4), (2.5) can be obtained. Without losing generality we may assume an exponential dependence on y and on t and write the solution in the form

$$v = \sum_{n=1}^{4} A_j \exp\{-\mu_j x + \mathrm{i}\beta y + \mathrm{i}\tilde{\omega}t\} \sin \pi z, \tag{2.6a}$$

$$\theta = \sum_{j=1}^{4} B_j \exp\{-\mu_j x + \mathrm{i}\beta y + \mathrm{i}\tilde{\omega}t\} \cos \pi z, \tag{2.6b}$$

$$w = \sum_{j=1}^{4} C_j \exp\{-\mu_j x + \mathrm{i}\beta y + \mathrm{i}\tilde{\omega}t\} \cos \pi z, \tag{2.6c}$$

where the constants μ_j are the roots with positive real part of the equation

$$\hat{q}(\hat{q} - \mathrm{i}\tilde{\omega}/P)^2(\hat{q} - \mathrm{i}\tilde{\omega}) - R(\hat{q} - \mathrm{i}\tilde{\omega}/P)(\hat{q} + \pi^2) - \tau^2\pi^2(\hat{q} - \mathrm{i}\tilde{\omega}) = 0, \tag{2.7}$$

with

$$\hat{q} \equiv \mu^2 - \beta^2 - \pi^2,$$

which follows from (2.2). Once the roots μ_j have been determined, the coefficients A_j, B_j, C_j can be obtained in terms of four unknowns $D_j, j = 1, \ldots, 4$,

$$A_j = (\beta^2 R - (\beta^2 + \pi^2)(\hat{q}_j - \mathrm{i}\tilde{\omega}/P)(\hat{q}_j - \mathrm{i}\tilde{\omega}))\, D_j, \tag{2.8a}$$

$$B_j = (\beta^2 + \pi^2)(\mathrm{i}\beta\tau\pi - \mu_j \pi(\hat{q}_j - \mathrm{i}\tilde{\omega}/P))\, D_j, \tag{2.8b}$$

$$C_j = (\mathrm{i}\beta R\mu_j \pi + \tau\pi(\beta^2 + \pi^2)(\hat{q}_j - \mathrm{i}\tilde{\omega}))\, D_j, \tag{2.8c}$$

with

$$\hat{q}_j \equiv \mu_j^2 - \beta^2 - \pi^2.$$

The unknowns D_j are determined by the boundary conditions at $x = 0$,

$$\sum_{j=1}^{4} \hat{f}_j(\mathrm{i}\beta\tau\pi - \mu_j\pi(\hat{q}_j - \mathrm{i}\tilde{\omega}/P))\, D_j = 0, \tag{2.9a}$$

$$\sum_{j=1}^{r} [\beta^2 R - (\beta^2+\pi^2)(\hat{q}_j - \mathrm{i}\tilde{\omega})(\hat{q}_j - \mathrm{i}\tilde{\omega}/P)]\, D_j = 0, \tag{2.9b}$$

$$\sum_{j=1}^{4} \mu_j[\beta^2 R - (\beta^2+\pi^2)(\hat{q}_j - \mathrm{i}\tilde{\omega})(\hat{q}_j - \mathrm{i}\tilde{\omega}/P)]\, D_j = 0, \tag{2.9c}$$

$$\sum_{j=1}^{4} [\mathrm{i}\beta R\mu_j\pi + \tau\pi(\beta^2+\pi^2)(\hat{q}_j - \mathrm{i}\tilde{\omega})]\, D_j = 0, \tag{2.9d}$$

where $$\left.\begin{matrix}\hat{f}_j = \mu_j \\ \hat{f}_j = 1\end{matrix}\right\} \quad \text{for } j = 1,\ldots,4 \text{ in the case } \left\{\begin{matrix}\mathrm{I}\\ \mathrm{C}\end{matrix}\right\}. \tag{2.10}$$

The solvability of the system (2.9) of homogeneous equations requires that the determinant of the coefficient matrix vanishes. In the following we shall first evaluate the determinant in the limit of large τ and then compare the results with a numerical solution at moderate values of τ.

3. Asymptotic analysis

In the limit of large τ it is convenient to use rescaled quantities,

$$r \equiv \lambda^4 R, \quad \omega \equiv \lambda^2\tilde{\omega}, \quad \nu_j \equiv \lambda\mu_j, \quad q_j \equiv \nu_j^2 - \lambda^2(\beta^2+\pi^2), \quad j = 1,\ldots,4, \tag{3.1a}$$

where λ is defined by $$\lambda \equiv (\tau\pi)^{-\frac{1}{3}}. \tag{3.1b}$$

Accordingly (2.7) for the roots q_j can be written in the form

$$q_j\left(q_j - \frac{\mathrm{i}\omega}{P}\right)^2 (q_j - \mathrm{i}\omega) - r\left(q_j - \frac{\mathrm{i}\omega}{P}\right)(q_j + \lambda^2\pi^2) - q_j + \mathrm{i}\omega = 0 \quad \text{for } j = 1,\ldots,4, \tag{3.2}$$

and the condition that the determinant of the homogeneous system (2.9) vanishes becomes

$$D \equiv \det \begin{vmatrix} f_1(\mathrm{i}\beta - \pi\nu_1(q_1 - \mathrm{i}\omega/P)) & \ldots \\ \beta^2 r - (\beta^2+\pi^2)(q_1 - \mathrm{i}\omega/P)(q_1 - \mathrm{i}\omega) & \ldots \\ \nu_1(\beta^2 r - (\beta^2+\pi^2)(q_1 - \mathrm{i}\omega/P)(q_1 - \mathrm{i}\omega)) & \ldots \\ \mathrm{i}\beta r\nu_1\pi + (\beta^2+\pi^2)(q_1 - \mathrm{i}\omega) & \ldots \end{vmatrix} = 0, \tag{3.3}$$

where the dots indicate the same columns as the first one except that the subscript 1 is replaced by 2, 3 and 4, respectively, and where f_i denotes the rescaled version of $\hat{f}_i$,

$$f_i = \left\{\begin{matrix}\nu_i \\ 1\end{matrix}\right\} \quad \text{in case} \quad \left\{\begin{matrix}\mathrm{I}\\ \mathrm{C}\end{matrix}\right\}. \tag{3.4}$$

The rescaling (3.1) has been motivated by the property that all terms in the coefficient matrix (3.3) are of the same order and an explicit dependence of (3.3) on λ has been eliminated. The real and imaginary parts of (3.3) determine r and ω as functions of β and λ. In the limit $\lambda = 0$ (3.3) can be evaluated easily in case I. The solution

$$r^{(0)} = \omega^{(0)} = 0, \quad q_1^{(0)} = \nu_1^{(0)} = 0, \quad (q_j^{(0)})^3 = 1 \quad \text{for} \quad j = 2,3,4 \tag{3.5}$$

satisfies (3.3) since the first column vanishes identically. Since ν_1 will be of order λ we introduce the perturbation expansion

$$\nu_1 = \lambda\nu_1^{(1)} + \ldots, \quad r = \lambda r^{(1)} + \lambda^2 r^{(2)} + \ldots, \quad \omega = \lambda\omega^{(1)} + \lambda^2\omega^{(2)} + \ldots \tag{3.6}$$

and obtain at order λ of (3.3) the condition

$$\begin{vmatrix} \mathrm{i}\nu_1^{(1)}\beta & \nu_2^{(0)}(\mathrm{i}\beta-\pi\nu_2^{(0)}q_2^{(0)}) & \dots \\ \beta^2 r^{(1)} & -(\beta^2+\pi^2)(q_2^{(0)})^2 & \dots \\ 0 & -\nu_2^{(0)}(\beta^2+\pi^2)(q_2^{(0)})^2 & \dots \\ 0 & (\beta^2+\pi^2)\,q_2^{(0)} & \dots \end{vmatrix} = 0 \tag{3.7}$$

where the third and fourth columns are identical to the second one except that the subscript 2 is replaced by 3 and 4, respectively. To obtain a consistent expression for $\nu_1^{(1)}$, we must require $\omega^{(1)} = 0$ with the result

$$\nu_1^{(1)} = (\beta^2+\pi^2+\mathrm{i}\omega^{(2)})^{\frac{1}{3}}. \tag{3.8}$$

After rewriting (3.6) in the form

$$2\beta(\beta^2+\pi^2)^2(\mathrm{i}\beta+\pi)(\nu_4^{(0)}-\nu_3^{(0)})(\nu_1^{(1)}(\beta+\mathrm{i}\pi)-\beta r^{(1)}) = 0,$$

where the convention $q_2^{(0)} = 1$ has been used, we obtain

$$r^{(1)} = (\beta^2+\pi^2+\mathrm{i}\omega^{(2)})^{\frac{1}{3}}(1+\mathrm{i}\pi/\beta). \tag{3.9}$$

Equating real and imaginary parts in this relationship we find

$$\omega^{(2)} = -2\beta\pi\frac{\beta^2+\pi^2}{\beta^2-\pi^2}, \quad (r^{(1)})^2 = \frac{(\beta^2+\pi^2)^3}{\beta^2(\beta^2-\pi^2)}. \tag{3.10}$$

The positive minimum of $(r^{(1)})^2$ is obtained for

$$r_c^{(1)} = \pi(6\sqrt{3})^{\frac{1}{3}}, \quad \beta_c = \pi(2+\sqrt{3})^{\frac{1}{3}}, \quad \omega_c^{(2)} = -2\pi\sqrt{3}\,\beta_c. \tag{3.11}$$

The conditions for the onset of wall-attached convection are thus given for large τ in the case of an insulating wall by

$$R_c = \pi^2(6\sqrt{3})^{\frac{1}{2}}\tau, \quad \beta_c = \pi(2+\sqrt{3})^{\frac{1}{3}}, \quad \tilde{\omega}_c = -2\pi\sqrt{3}\,\beta_c. \tag{3.12}$$

Since the wave-like convection modes propagate in the positive y-direction, they propagate against the sense of rotation inside a cylindrical wall with an axis parallel to the axis of rotation, and with the sense of rotation if the fluid is outside such wall.

The analysis of the problem posed by (3.3) together with relationship (3.2) becomes more complex in the case of a conducting sidewall. When one tries to obtain a solution for $\lambda = 0$ with $\omega = 0$ one finds that the real part of the determinant does not vanish unless the limit of large β is approached. In this limit the determinant can be written in the form

$$D = -\mathrm{i}\beta^7\begin{vmatrix} 1 & 1 & 1 & 1 \\ r & -q_2^{-1} & -q_3^{-1} & -q_4^{-1} \\ 0 & \nu_2 q_2^{-1} & \nu_3 q_3^{-1} & \nu_4 q_4^{-1} \\ 0 & q_2 & q_3 & q_4 \end{vmatrix} = 0, \tag{3.13}$$

which corresponds to some high-order polynomial in r because of the relationship $q_j^3 - rq_j - 1 = 0$. A numerical determination of the lowest root yields

$$r^{(0)} = 0.908\,560\,3. \tag{3.14}$$

The high wavenumber β that is obviously required for the onset of convection suggests a scaling of the form $\alpha = \beta\lambda^{-\gamma}$. When an expansion similar to (3.6) but with λ^δ instead of λ is introduced, a consistent balance is found for $\gamma = \delta = \frac{1}{2}$. We thus start with the expansion

$$\left.\begin{aligned} \nu_j = \nu_j^{(0)} + \lambda^{\frac{1}{2}}\nu_j^{(1)} + \dots, \quad \omega = \omega^{(0)} + \lambda^{\frac{1}{2}}\omega^{(1)} + \lambda\omega^{(2)} + \dots, \\ r = r^{(0)} + \lambda^{\frac{1}{2}}\lambda r^{(1)} + \dots, \quad \alpha = \lambda^{\frac{1}{2}}\beta, \end{aligned}\right\} \tag{3.15}$$

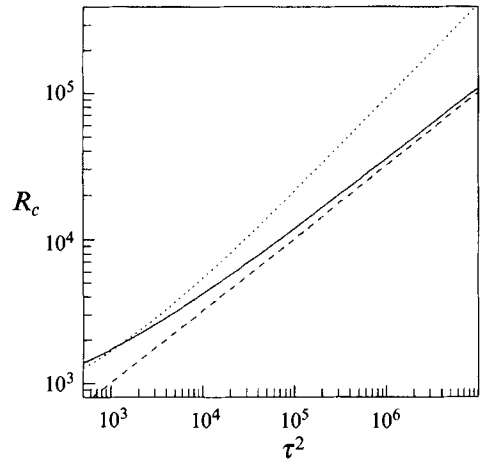

FIGURE 2. The critical Rayleigh number R_c for the onset of convection at an insulating wall as a function of $\tau^2 = \Omega^2 d^2/\nu^2$ as obtained from numerical calculations (solid line) in comparison with the asymptotic value (3.12) (dashed line) and the value for an infinite layer (dotted line).

and obtain at order λ^{-3} of the determinant

$$\alpha^6 \begin{vmatrix} 0 & -\nu_2^{(0)} q_2^{(0)} \pi & \dots \\ r^{(0)} & -(q_2^{(0)})^{-1} & \dots \\ 0 & -\nu_2^{(0)}(q_2^{(0)})^{-1} & \dots \\ 0 & q_2^{(0)} & \dots \end{vmatrix} + \alpha^7 \begin{vmatrix} \mathrm{i} & \mathrm{i} & \dots \\ r^{(1)} & r^{(1)} - 2q_2^{(0)} q_2^{(1)} & \dots \\ 0 & -\nu_2^{(0)}(q_2^{(0)})^{-1} & \dots \\ 0 & q_2^{(0)} & \dots \end{vmatrix}$$

$$+ \alpha^7 \begin{vmatrix} \mathrm{i} & \mathrm{i} & \dots \\ r^{(0)} & -(q_2^{(0)})^{-1} & \dots \\ \nu_1^{(0)} r^{(0)} & S_2 & \dots \\ 0 & q_2^{(0)} & \dots \end{vmatrix} + \alpha^7 \begin{vmatrix} \mathrm{i} & \mathrm{i} & \dots \\ r^{(0)} & -(q_2^{(0)})^{-1} & \dots \\ 0 & -\nu_2^{(0)}(q_2^{(0)})^{-1} & \dots \\ 0 & q_2^{(1)} + \mathrm{i}\alpha^{-1} r^{(0)} \nu_2^{(0)} \pi & \dots \end{vmatrix} = 0, \quad (3.16)$$

where the second column is repeated in the third and fourth columns of each determinant with the subscript 2 replaced by 3 and 4, respectively, and where the abbreviation

$$S_j \equiv \nu_j^{(0)}(r^{(0)} - 2q_j^{(0)} q_j^{(1)}) + \nu_j^{(1)}(r^{(0)} - (q_j^{(0)})^2)$$

has been used. As in case I, $\omega^{(1)}$ must vanish and the quantities $\nu_j^{(1)}$ are given by

$$\nu_1^{(1)} = (\alpha^2 + \mathrm{i}\omega^{(2)})^{\frac{1}{2}}, \quad \nu_j^{(1)} = r^{(1)}(q_j^{(0)})^{\frac{3}{2}}[4(q_j^{(0)})^3 + 2]^{-1} \quad \text{for} \quad j = 2, 3, 4. \quad (3.17)$$

An inspection of (3.16) shows that it can be written in the form

$$\alpha^6\{\alpha(-Er^{(1)} + F\nu_1^{(1)}) + \mathrm{i}G\} = 0, \quad (3.18)$$

where E, F and G are real numbers which can be computed numerically,

$$E = 5.00740, \quad F = 4.45102, \quad G = 12.70466. \quad (3.19)$$

The separation of the wavy bracket in (3.18) into real and imaginary parts yields

$$\omega^{(2)} = \pm 2\left[\left(\frac{G}{F}\right)^2 + \alpha^{-4}\left(\frac{G}{F}\right)^4\right]^{\frac{1}{2}} \quad \text{and} \quad r^{(1)} = -\frac{F^2}{2EG}\alpha\omega^{(2)}. \quad (3.20)$$

Since we assume a positive wavenumber α, the negative sign of $\omega^{(2)}$ must be chosen in order to obtain a finite minimum for $r^{(1)}$. Since $r^{(0)}$ is independent of β, the minimum of R is determined by $\partial r^{(1)}/\partial\alpha = 0$. This condition yields

$$\alpha_c = (G/F)^{\frac{1}{2}}, \quad \omega_c^{(2)} = 2\sqrt{2G/F}, \quad r_c^{(1)} = (2GF)^{\frac{1}{2}}/E. \quad (3.21)$$

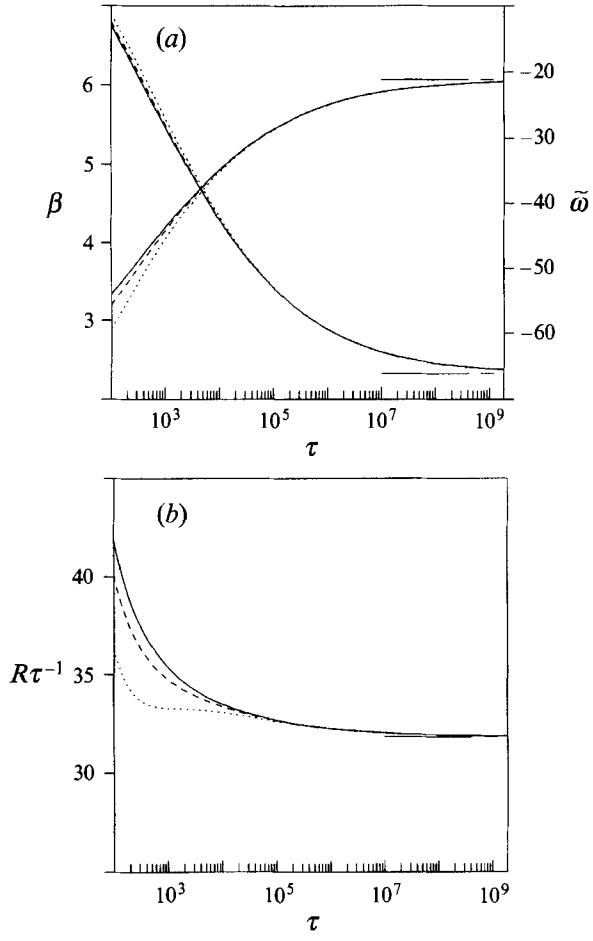

FIGURE 3. (*a*) The critical wavenumber β_c (ascending lines, left ordinate) and the critical frequency $\tilde{\omega}_c$ (descending lines, right ordinate) for Prandtl numbers 7.0 (solid lines), 2.0 (dashed lines), and 0.7 (dotted lines). The long dash-short dash lines indicate the asymptotic values. (*b*) The scaled critical Rayleigh number for the same parameters as used in (*a*).

Using the numerical values for E, F and G we obtain the following asymptotic critical conditions for the onset of convection attached to a conducting sidewall:

$$\beta_c = 1.689(\tau\pi)^{\frac{1}{6}} + o(1), \tag{3.22a}$$

$$\tilde{\omega}_c = -8.073(\tau\pi)^{\frac{1}{3}} + o(\tau^{\frac{1}{6}}), \tag{3.22b}$$

$$R_c = 0.9086(\tau\pi)^{\frac{4}{3}} + 2.124(\tau\pi)^{\frac{7}{6}} + o(\tau). \tag{3.22c}$$

4. Comparison with numerical results

In the numerical investigation the full problem posed by (3.2) and (3.3) is solved. No special difficulty is encountered when the problem is attacked with the usual library routines on a computer except for the property that a solution cannot be obtained for low values of τ, where a wall-attached convection mode is no longer feasible. In figure 2 the strong reduction of the critical Rayleigh number for the onset of convection near an insulating wall can be seen. For values of τ as low as 10^3 the asymptotic expression

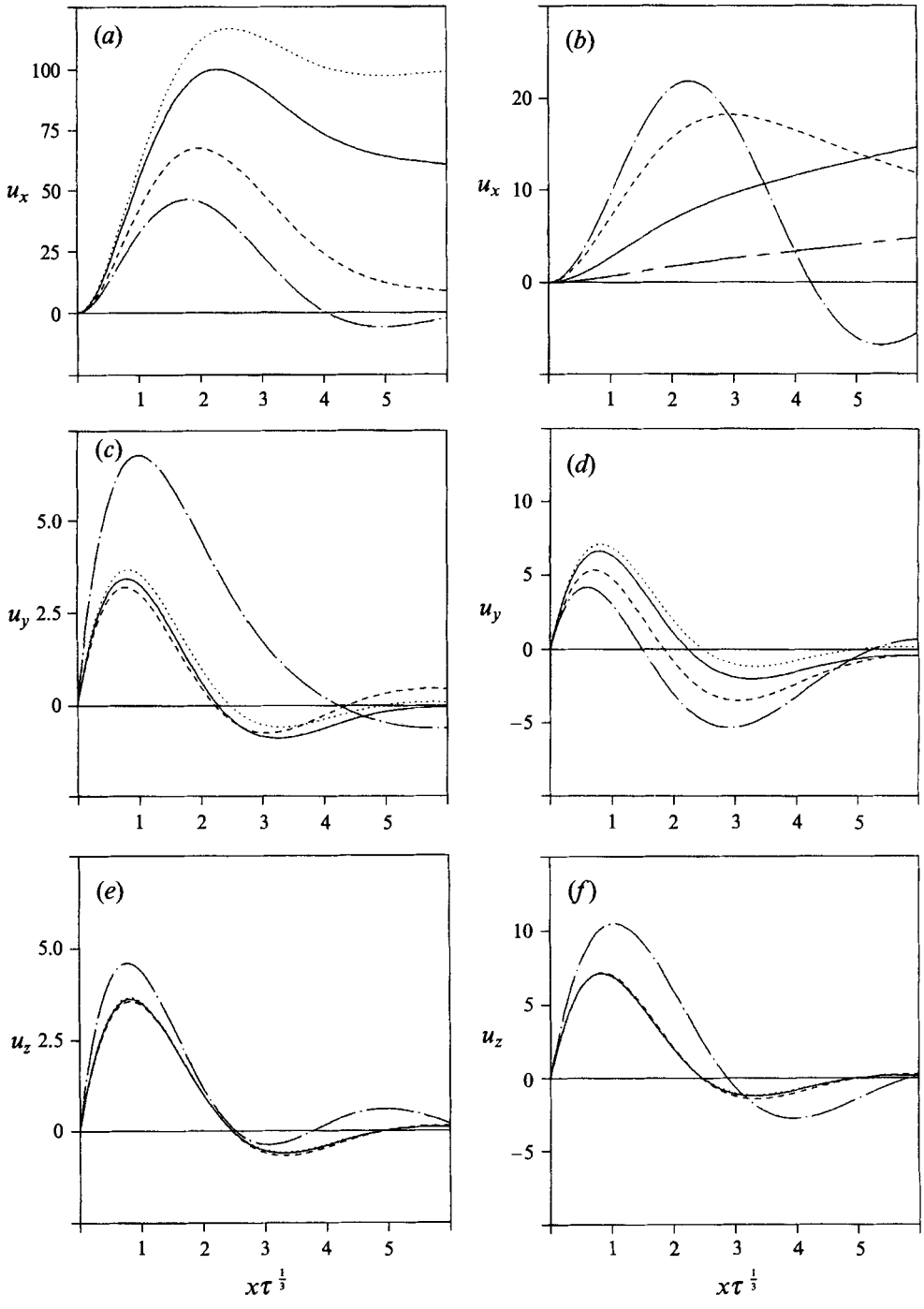

FIGURE 4. (*a*) Real part of the normal velocity $u_x \equiv -\Delta_2 v$ as a function of the scaled distance from the sidewall for $\tau = 10^2$ (dash-dotted line), $\tau = 10^4$ (dashed line), $\tau = 10^6$ (solid line), and the asymptotic case, $\tau = \infty$ (dotted line). $P = 7.0$ has been assumed. (*b*) Same as (*a*) but for the imaginary part of u_x. Instead of the asymptotic case, the case $\tau = 10^8$ (long dash-short dash line) has been plotted. (*c*) Same as (*a*) but for $u_y \equiv \tau^{-\frac{1}{3}}(\partial^2 v/\partial x\,\partial y + \partial w/\partial z)$. (*d*) Same as (*c*) but for the imaginary part of u_y. (*e*) Same as (*c*) but for $u_z \equiv \tau^{-\frac{1}{3}}(\partial^2 v/\partial x\,\partial z - \partial w/\partial y)$ instead of u_y. (*f*) Same as (*e*) but for the imaginary part of u_z.

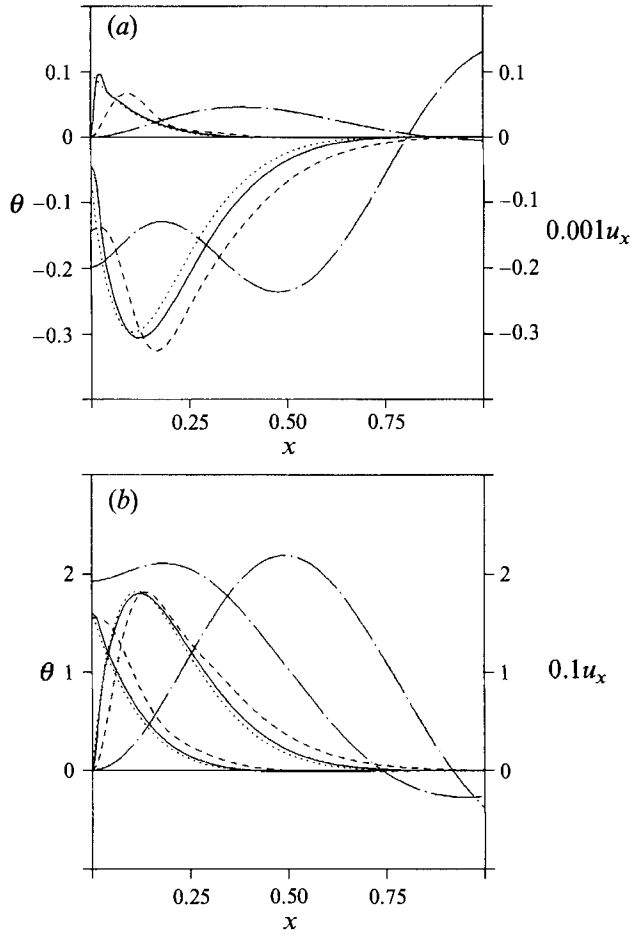

FIGURE 5. (*a*) Real parts of the temperature θ and of u_x (positive curves) as a function of the distance x from the wall for $\tau = 10^2$ (dash-dotted lines), $\tau = 10^4$ (dashed lines), $\tau = 10^6$ (solid lines), and for the asymptotic case $\tau = \infty$ (dotted line). $P = 7.0$ has been assumed. (*b*) Same as (*a*) but for the imaginary parts. The lines of u_x start at zero for $x = 0$.

(3.12) is already within 5% of the numerically determined value. The approach towards the asymptotic value is less rapid for the wavenumber β and the frequency $\tilde{\omega}$ as shown in figure 3. It is remarkable to see, however, the small influence of the Prandtl number. The property of vanishing Prandtl-number dependence of the asymptotic results is thus modified only slightly for finite values of τ.

In figures 4 and 5 the three components of the velocity field and the temperature disturbance are plotted. The components parallel to the wall are restricted to a layer with a thickness of order $\tau^{-\frac{1}{3}}$ while the normal velocity component and the temperature disturbance include contributions which extend to a distance of order unity from the boundary. The latter dependence is of the order $\exp\{-\beta x\}$. In the case of a conducting boundary, the corresponding terms will thus decay much faster with distance from the wall.

The solutions shown in the plots of figure 4 have been normalized in such a way that the $\exp\{-\mu_1 x\}$ term of u_x has the amplitude 100 at the wall. The lines of vanishing u_x assume an angle of 34° with the x-axis and are directed in the negative y-direction at distances of order unity from the wall. The roll-like structure with an exponential decay

away from the boundary shows some similarity with the phenomenon of Kelvin waves. The propagation of wall-attached convection is similar to that of Kelvin waves, except for the opposite sense with respect to the axis of rotation. The main difference lies in the dominance of dissipative processes in the case of convection, which are not important for Kelvin waves.

The support of the sidewall for the onset of convection depends primarily on its thermal properties. Because a conducting sidewall tends to damp the temperature perturbation, much less buoyancy is available to counteract the effects of viscous friction and of the stabilizing Coriolis force. As shown in figure 6 the deviations from the case of an infinite layer are much reduced. As in the case of the insulating wall the approach towards the asymptotic expressions is much faster for R_c than for $\tilde{\omega}_c$ and β_c.

5. Concluding remarks

The phenomenon of wall-attached convection appears to be a unique property of rotating systems. In non-rotating systems sidewalls in general exert a stabilizing influence on the onset of convection unless they disturb in some way the basic state of pure heat conduction. The steady mode of convection in an infinitely extended rotating layer also appears to be slightly stabilized by the presence of sidewalls. In their analysis of the onset of convection in a circular layer, Goldstein *et al.* (1993) do indeed distinguish two modes of convection. Besides the wall-attached mode there is a roll-like convection pattern growing from the centre towards the walls which exhibits a much slower drift than the wall-attached mode. The interesting nonlinear interactions visible in the experimental study (Zhong *et al.* 1991) should be accessible to a weakly nonlinear analysis of the problem.

The curvature of the sidewall exerts only a secondary influence on the onset of convection as is evident from the comparison with the results of Goldstein *et al.* (1993) which have been computed for a cylindrical box with its height equal to its radius. Using the integer value β corresponding to the wavelength of the convection pattern at the rim of the box we obtain slightly higher values for Rayleigh numbers and frequencies. But a rapid convergence with increasing τ can be seen in table 1. The difference between the values for $\Gamma = 1$ and ∞ can be explained in part by the fact that the effective wavenumber in the case $\Gamma = 1$ is higher since it characterizes convection at some distance from the sidewall. For the cases $\tau = 40$ and 100 an increase of β yields lower values for R and $\tilde{\omega}$ as can be seen from the critical values for $\Gamma = \infty$ which also have been listed in table 1. There remains, however, a destabilizing effect of the curvature of the sidewalls as is evident from the data for $\tau = 500$ where the integer value $\beta = 4$ closely matches the critical value β_c for $\Gamma = \infty$.

The drifting wall-attached convection must be clearly distinguished from the oscillatory onset of convection expected in the case of low-Prandtl-number fluids. The latter type of convection exhibits the dynamical properties of inertial oscillations and the frequency is thus of the order of the angular velocity Ω of rotation. The critical Rayleigh number for the onset of oscillatory convection in an infinite layer grows in proportion to $(P\tau)^{\frac{4}{3}}$ for low P according to Chandrasekhar (1961). The convection mode attached to an insulating wall considered in the present paper is thus still preferred if the rotation rate is sufficiently high according to relationships (3.12). The convection mode attached to a conducting wall, however, will be preferred only for $P \geqslant 0.37$ at high rotation rates.

After this paper had been submitted a paper by Kuo & Cross (1993) became known, in which the same problem is analysed independently. Their results agree with those of

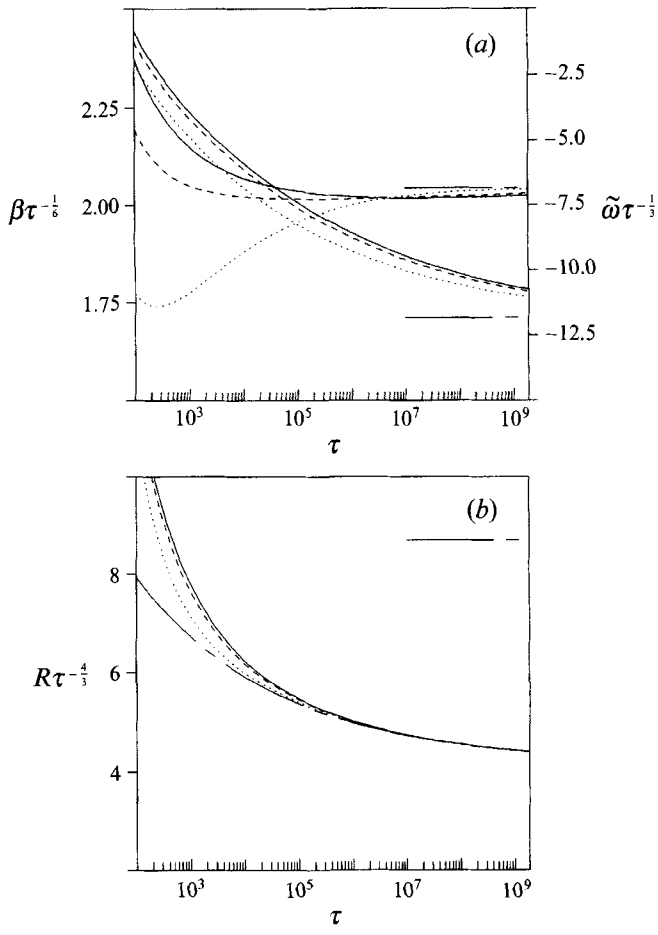

FIGURE 6. (*a*) The critical wavenumber β (ascending lines for large τ, left ordinate) and the critical frequency $\tilde{\omega}$ (descending lines for large τ, right ordinate) for $P = 7.0$ (solid line), $P = 2.0$ (dashed line), and $P = 0.7$ (dotted line). The constant lines indicate the asymptotic values given by (3.22*a*, *b*). (*b*) The critical Rayleigh number R_c for the onset of convection at a conducting wall for the same cases as in (*a*). The long dash-short dash line indicates the asymptotic expression (3.22*c*) and the constant line indicates the asymptotic value for an infinite layer.

		$\Gamma = 1$		$\Gamma = \infty$				
τ	β	R_c	$\tilde{\omega}_c$	R_0	$\tilde{\omega}_0$	β_c	R_c	$\tilde{\omega}_c$
40	2	1990.26	8.68	2248.5	9.89	3.006	2014.5	7.01
100	3	3945.30	12.22	4215.6	13.71	3.332	4181.0	12.79
500	4	17260.48	22.69	18203.9	23.46	3.936	18199.8	23.60
1000	5	34989.6	26.88	36318.6	27.05	4.191	35347.3	28.29

TABLE 1. Comparison of critical Rayleigh numbers R_c and frequencies $\tilde{\omega}_c$ in the case of a circular cylinder with radius 1, i.e. $\Gamma = 1$, calculated by Goldstein *et al.* (1993) with values R_0, $\tilde{\omega}_0$ of the present analysis corresponding to the limit of an infinite radius, $\Gamma = \infty$, for the same wavenumber β. Also shown are the critical values for $\Gamma = \infty$. $P = 6.7$ has been used for all computations except for the case $\tau = 1000$ where $P = 7.0$ has been used. In this latter case the critical wavenumber for $\Gamma = 1$ is $\beta = 4$, but accurate numerical values have been given by Goldstein *et al.* (1993) only for $\beta = 5$.

the present paper in the case of the insulating sidewall. Explicit results for the case of an infinitely conducting sidewall and details on the convection modes have not been given in their paper.

The main results of the present paper have been presented at Workshop on Mixing in Geophysical Flows, Dec. 16–18, 1992, Barcelona, Spain. The support of the Deutsche Forschungsgemeinschaft under Grant BU 589/2 is gratefully acknowledged.

REFERENCES

BUELL, J. C. & CATTON, I. 1983 Effect of rotation on the stability of a bounded cylindrical layer of fluid heated from below. *Phys. Fluids* **26**, 892–896.

CHANDRASEKHAR, S. 1961 *Hydrodynamic and Hydromagnetic Stability*. Clarendon.

ECKE, E. R., ZHONG, F. & KNOBLOCH, E. 1992 Hopf bifurcation with broken reflection symmetry in rotating Rayleigh–Bénard convection. *Europhys. Lett.* **19**, 177–182.

GOLDSTEIN, H. F., KNOBLOCH, E., MERCADER, I. & NET, M. 1993 Convection in a rotating cylinder. Part 1. Linear theory for moderate Prandtl numbers. *J. Fluid Mech.*

KUO, E. Y. & CROSS, M. C. 1993 Travelling-wave wall states in rotating Rayleigh–Bénard convection. *Phys. Rev.* E **47** R2245–2248.

LUCAS, P. G. J., PFOTENHAUER, J. M. & DONNELLY, R. J. 1983 Stability and heat transfer of rotating cryogens. Part 1. Influence of rotation on the onset of convection in liquid ^{4}He. *J. Fluid Mech.* **129**, 251–264.

PFOTENHAUER, J. M., NIEMELA, J. J. & DONNELLY, R. J. 1987 Stability and heat transfer of rotating cryogens. Part 3. Effects of finite cylindrical geometry and rotation on the onset of convection. *J. Fluid Mech.* **175**, 85–96.

ROSSBY, H. T. 1969 A study of Bénard convection with and without rotation. *J. Fluid Mech.* **36**, 309–335.

ZHONG, F., ECKE, R. E. & STEINBERG, V. 1991 Asymmetric modes and the transition to vortex structures in rotating Rayleigh–Bénard convection. *Phys. Rev. Lett.* **67**, 2473–2476.